

SCATTERING OF LASER RADIATION

PACS numbers: 42.25.Fx; 82.70.-y
DOI: 10.1070/QE2005v035n02ABEH002898

Small-angle scattering of laser radiation by stable micron particles in twice-distilled water

N.F. Bunkin, N.V. Suyazov, D.Yu. Tsipenyuk

Abstract. **Small-angle scattering of laser radiation in purified (twice-distilled) water is studied experimentally. The scattering indicatrix shows that such water contains scattering micron impurities. The parameters of the size distribution of these impurities are estimated from the experimental data. The results obtained in the paper confirm the earlier proposed hypothesis about the presence of stable microbubbles of gas, bubstons, dissolved in pure liquids.**

Keywords: *small-angle scattering of laser radiation, Mie scattering, colloidal particles in liquids.*

1. Introduction

Small-angle scattering of light is a powerful tool for studying the parameters of suspended particles in liquids. This problem has been extensively discussed in the literature, therefore, not claiming the comprehensive citation of papers devoted to this topic, we will mention here only the monograph [1] where numerous experimental schemes are presented and many papers are cited in the second chapter. Note that although this book was published in 1976, the basic principles of the design of setups for studying small-angle scattering of light in liquids have not been changed substantially so far, all the devices being based on the operation principle of a laser goniometer. Let us also point out the specific features of experiments on small-angle scattering of light (at an angle less than 0.1°), which occurs when scattering particles are quite large, i.e., the scattering indicatrix is predominantly directed forward and demonstrates the anisotropic properties of particles. In this case, instead of a goniometer a detector array (multichannel detection system) located in the focal plane of a lens can be used, where the scattering angle is related to the geometrical position of a given detector in the array [2]. Another scheme [3] uses a photomultiplier (one-channel detection scheme) located in the focal plane of a lens instead of a detector array. The input window of the photomultiplier has a diaphragm of diameter 50 μm, and the photomultiplier can be displaced in this plane, i.e., the position of the diaphragm in the focal plane determines the scattering angle.

Therefore, we see that the study of small-angle scattering is based on the measurement of the intensity distribution of scattered radiation in the focal plane of the lens. The lens serves as a dispersion element (with respect to the angular spectrum) collecting the beams scattered at a certain angle to concentric circles in the focal plane of the lens (obviously, the focus itself is the centre of these circles). Because the focusing quality in the focal plane is impaired with increasing scattering angle (i.e., as the angle of incidence of light on the lens increases), it is necessary to determine preliminary the angular range where this scheme can be used. In the case of large scattering angles, a usual goniometer should be used.

Our interest in experiments on small-angle scattering was stimulated by the appearance of theoretical models and experimental results demonstrating the existence of the microphase of bubbles of a dissolved gas, the so-called bubstons, in purified water under normal conditions. The nucleation and stabilisation of bubstons by ions in the liquid were theoretically interpreted in papers [4 – 6], and it was shown [7 – 9] that bubstons serve as nuclei of the optical breakdown in a transparent liquid. We mention here also paper [10], where bubstons were shown to affect the short-range-order structure in liquid, and recent paper [11] where the existence of bubstons was proved in the acoustic cavitation experiment. It was confirmed theoretically and experimentally in [4 – 9] that bubstons are capable of coagulation accompanied by the formation of bubston clusters. Note that such clusters are of micron size, i.e., these particles should scatter light at small angles in the optical wavelength range. Therefore, the characteristic size of bubston clusters and their distribution functions can be found in experiments on small-angle scattering of light in twice-distilled water saturated with a dissolved gas. The first experiments in this field were performed in [12] and then continued in [13].

This paper is a continuation of our small-angle scattering studies of the properties of suspended particles in the optical range.

2. Experimental

Our simplest experiment was the observation with a microscope of radiation scattered perpendicular to a 0.53-μm laser beam of diameter 1 mm propagating through a cell with twice-distilled water. The scattering pattern exhibits bright dots against a weak background of molecular

N.F. Bunkin, N.V. Suyazov, D.Yu. Tsipenyuk Wave Research Center, A.M. Prokhorov General Physics Institute, Russian Academy of Sciences, ul. Vavilova 38, 119991 Moscow, Russia

Received 1 October 2004; revision received 16 November 2004
Kvantovaya Elektronika **35** (2) 180 – 184 (2005)
Translated by M.N. Sapozhnikov

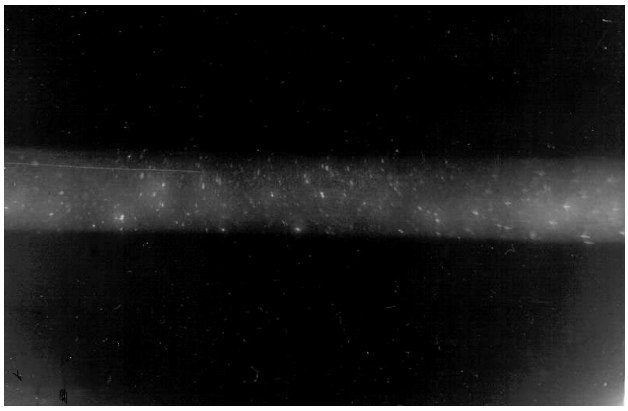

Figure 1. Optical-microscope photograph of scatterers in twice-distilled water.

scattering (Fig. 1). The localisation of these dots in the laser beam is determined by the depth of focus of the microscope. This fact suggests that the concentration of micron scatterers in twice-distilled, passed through an ion-exchange resin column, and long settled water is noticeable. The specific resistance of such water is 8 MΩ cm.

These scatterers were investigated in more detail in thoroughly purified water by the method of small-angle scattering. The main difference of our experimental scheme from those mentioned above was that the liquid was studied in a semicylindrical cell, which simultaneously served as a focusing system (Fig. 2). Such a combined scheme allows one to use a larger scattering volume due to milder restrictions imposed by a paraxial scattered beam. The output window of the semicylindrical cell was half the Pyrex cylinder of radius $r = 6$ cm cut along its axis and glued to a rough textolite plate. The plate had a hole of radius $r_0 = 0.3$ cm, to which a Pyrex plate (input window) in the form of an optical wedge was glued outside. The output window (Pyrex semicylinder) was also polished to form a 'wedge' (cylindrical) to avoid optical interference from the input and output windows. The use of the rough textolite plate allowed us to minimise flares on the input surface caused by the reflection of the incident beam from the output window. Note also that there was no reason to think that the textolite surface could additionally contaminate the liquid.

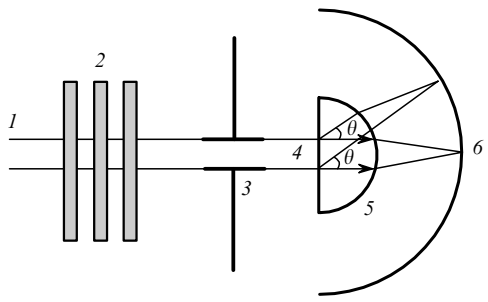

Figure 2. Scheme of the experimental setup: (*1*) laser beam; (*2*) optical filters; (*3*) diaphragm; (*4*) input window of a cell with liquid under study; (*5*) output window of a cell with liquid under study; (*6*) reflecting screen (photographic camera is located over the cell and is not shown).

Such a cell filled with liquid (experiments were performed with twice-distilled water) became a cylindrical lens. The focal point was located at the distance

$$a = \frac{rn}{n-1} \tag{1}$$

from the lens axis, where n is the reflective index of water (in our case, $n = 1.33$ and $a = 24$ cm). The distance a was determined experimentally each time and corresponded to expression (1).

With this cell filled with water, we determined the scattering indicatrix within a certain range of angles θ by measuring the distribution of scattered radiation along a screen in the form of a semicircumference of radius $r_1 = a$. The angular divergence of our laser beam was of the order of 10^{-3} rad, which, taking its paraxial nature into account ($r_0/r \ll 1$), provided the measurement of the scattering indicatrix in the angular range $\theta \leqslant 10^\circ$. The screen should provide the absence of any flares during photographing to obtain the intensity distribution of scattered radiation. The absence of flares was confirmed by the absence of 'splashes' in the scattering pattern and its symmetry with respect to the optical axis. After many preliminary experiments, we selected an aerial film as the screen, which was fixed so that the light was incident on its emulsion. The reflectivity of such a screen for scattered radiation was sufficient for photographing, and its drastic decrease at the site of incidence of direct laser radiation (darkening) was insignificant for our measurements.

The experimental setup is shown in Fig. 2. 0.53-μm, 50-mW second-harmonic radiation beam (*1*) from a cw single-mode Nd^{3+} : YAG laser (with the divergence 3×10^{-3} rad and the $1/e^2$-radius 1 mm) was attenuated with a set of neutral optical filters (*2*) passed through iris diaphragm (*3*), which rejected the light scattered by filters, and was incident on the input window of cell (*4*). Behind output window (*5*) reflecting screen (*6*) – a cylindrical surface with the radius of curvature calculated from (1) was located. A Casio QV-R40 digital camera (not shown in the figure) equipped with a 4-megapixel CCD array and an 8-bit ADC was mounted over the cell. The centre of the camera objective was located at a distance of 3 cm from the beam axis. This arrangement excluded aspect-angle effects. The camera recorded scattered radiation reflected from the screen, the recorded frames being computer processed. The electronic sensitivity of the camera, the diaphragm diameter, the exposure, and the focal distance of the objective could be varied.

Note that our experimental setup, unlike those used in papers [1 – 3], allows us to perform measurements simultaneously at very small angles (near the optical axis) and at angles of the order of 10° without changing the setup components.

Before the measurements of scattered radiation, the camera was calibrated by using a photodiode operating at a wavelength of 0.53 μm in the range from 10 μW to 1 W. The laser radiation (in the absence of the cell with liquid) was attenuated with a set of identical neutral optical filters of the same thickness. The measured power was normalised to the beam cross-section area to give the dependence of the radiation intensity I on the number k of filters used in the setup. According to the Bouguer law,

$$I = A\exp(-bk), \tag{2}$$

where A and b are constants calculated with a computer, based on the photodiode readings. The same radiation attenuated by optical filters was incident on the screen; radiation reflected from the screen was photographed and digitised. (The radiation was attenuated so that no darkening of the film occurred under the action of the incident light). Then, we determined the pixel-averaged digital signal of the 8-bit CCD array corresponding to the laser spot (altogether $2^8 = 256$ illumination gradations are possible). The dependence of the digital signal of the CCD array on the number k of optical filters has the form

$$I_1 = A_1 - b_1 k, \tag{3}$$

where A_1 and b_1 are computer-calculated constants. Therefore, the CCD array takes the logarithm of the incident radiation intensity. By finding the number k for (3) and substituting it into (2), we obtain

$$I = A\exp\left(-b\frac{A_1 - I_1}{b_1}\right), \tag{4}$$

which gives the unique relation between the digital signal I_1 of the CCD array, corresponding to radiation reflected from the screen, and the incident radiation intensity I.

To establish the relation between the number of the CCD array pixel and the scattering angle θ, we plotted a scale in angular degrees on the screen. The scale was calculated based on the focal distance of the cell with liquid. The photograph of this scale in usual room light and its subsequent digitising provided this relation.

The experimental results were processed as follows. First we digitised the two-dimensional scattering pattern and then found its maximum corresponding to direct (unscattered) radiation. The digitised direct radiation signal corresponds to complete saturation and is equal to 256 (in arbitrary units). The central pixel in the saturation region was selected and was related to the scattering angle $\theta = 0$. In addition, five lines were counted from this pixel upward and downward (each of them including approximately 2400 pixels) and averaging was performed over 10 lines. Then, the scattered radiation intensity was calculated from (4) and the dependence of this intensity on the scattering angle θ was plotted.

To perform quantitative measurements, we determined the instrumental function of our setup. For this purpose, the probe laser radiation (attenuated by optical filters) was transmitted through an empty cell, behind which a quartz cylindrical lens was placed to focus radiation to the same region on the screen as in the case of the cell with liquid. Figure 3a shows the dependence of the scattered radiation intensity I_s on the scattering angle θ for the empty cell with the lens. The experimental data are well fitted by the Gaussian dependence $I = I_0\exp[-(\theta/\theta_0)^2]$ for $\theta_0 = 0.33^\circ$, which corresponds to the effective divergence 4×10^{-3} rad. This value exceeds the laser beam divergence, which can be caused by diffraction from apertures in the setup and by scattering from cell walls and other inhomogeneities (in particular, by dust particles). The obtained value of θ_0 allows us to estimate the angular range near $\theta = 0$ in experiments on scattering in water which corresponds to the unscattered incident beam and is neglected in the measurement of the scattering indicatrix. We processed our results by assuming (with a margin) that the excluded interval was $|\theta| \leqslant 0.8^\circ$.

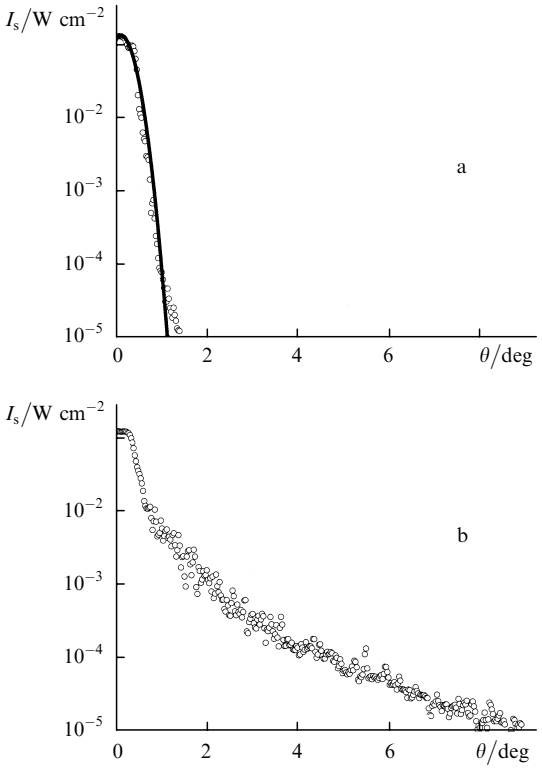

Figure 3. Angular dependences of the probe radiation intensity for an empty cell with a focusing lens located behind (a) and of the radiation intensity scattered in a semicylindrical cell with twice-distilled water (b).

3. Discussion of results

Figure 3b shows the angular dependence of the radiation intensity $I_s(\theta)$ scattered in a cell with twice-distilled water. Scattering in water results in a strong broadening of the angular dependence compared to that presented in Fig. 3a. To estimate the size of scatterers typical for water, we will use the so-called Guinier coordinates [14], i.e., consider the dependence of the measured values of I_s on the square of the scattering vector (Fig. 4),

$$q^2 = \left(\frac{4\pi n}{\lambda}\sin\frac{\theta}{2}\right)^2 \approx \left(\frac{2\pi n\theta}{\lambda}\right)^2, \tag{5}$$

where $\lambda = 0.53$ μm is the laser radiation wavelength. Such a representation of the experimental results is convenient because upon scattering of light by spherical particles with the optical density that considerably differs from the density of the surrounding liquid, the intensity of small-angle scattering caused mainly by diffraction is described by the relation (see, for example, [15])

$$I_s(q) = I_s(0)\left[\frac{2J_1(qR)}{qR}\right]^2, \tag{6}$$

where $I_s(0)$ is the intensity of radiation scattered at the angle $\theta = 0$; R is the scatterer radius; J_1 is the first-order

Bessel function of the argument qR. For small arguments ($qR < 2$), the second term in (6) can be replaced by $\exp[-(q^2R^2)/4]$ and the scattered radiation intensity can be written in the form

$$I_s(q) \approx I_s(0) \exp\left(-\frac{q^2R^2}{4}\right). \quad (7)$$

Expression (7) can be also used for non-spherical particles with R replaced by the effective radius of a particle [14]. Therefore, according to (7), the initial region of the small-angle scattering indicatrix in the Guinier coordinates q^2, I_s is described by a straight line with the slope determined by the radius R of particles and is $R^2/4$.

Let us estimate the characteristic dimensions of scatterers in distilled water by separating nearly linear regions in Fig. 4a [14]. We will require that the approximation confidence coefficient

$$Q^2 = 1 - \frac{N^{-1}\sum_{i=1}^{N}(y_i - f_i)^2}{N^{-1}\sum_{i=1}^{N}(y_i - \bar{y})^2} \quad (8)$$

achieves its maximum upon dividing experimental data into such regions. Here, N is the number of points in the selected region; y_i is the experimental values of the intensity; f_i are the values of the function in this region; $\bar{y}$ is the arithmetic mean calculated from experimental points in a given region; and the denominator of the fraction in (8) is dispersion. The maximum value $Q^2 = 1$ is achieved in this region in the case of the ideal approximation $y_i = f_i$. The results of heuristic division into linear regions are presented in Figs 4b–d.

The region in Fig. 4b completely lies in the excluded interval $|\theta| \leqslant 0.8^\circ$ and corresponds to direct (unscattered) radiation with the angular intensity distribution close to a Gaussian (Fig. 3a). Experimental points in selected regions in Figs 4c, d fall on the corresponding straight lines with the approximation confidence coefficient $Q^2 \approx 0.83$. This division seems optimal because a decrease (increase) in the number of regions, as well as their displacements along the abscissa and the addition of new regions (by reducing the initial ones) result in a decrease in Q^2. Therefore, we can make a preliminary conclusion within the framework of this model of date processing that twice-distilled water contains scatterers with characteristic sizes $R_1 \approx 3.7$ μm and $R_2 \approx 0.9$ μm. Note that the angular dependence of scattered radiation (Fig. 3b) has no minima, which are characteristic for scattering from particles with a fixed radius [14], as follows, for example, from (6). Within the framework of the model of spherical particles, such a situation is typical for a polydispersion medium with scatterers having the smooth size distribution function $p(R)$ and quite large dispersion. For example, for the two-parametric distribution

$$p(R) = 2R^g d^{-g-1} \frac{\exp(-R^2 d^{-2})}{\Gamma(g/2 + 1/2)} \quad (9)$$

of spherical particles with the scattering indicatrix (6), the dimensionless fitting parameter $g = 0.2$ and dimensional parameter $d = 4$ μm (Fig. 5b), the calculated angular dependence $I_s(\theta)$ is monotonic and approximates the experimental data in the region $0.8^\circ < \theta < 10^\circ$ with the confidence coefficient $Q^2 = 0.93$ (Fig. 5a). Note that the maximum of the distribution function in Fig. 5b corresponds to $R = 1.3$ μm. The characteristic radii obtained above can be used to estimate the range of distribution of spherical scatterers over radii. To refine this distribution

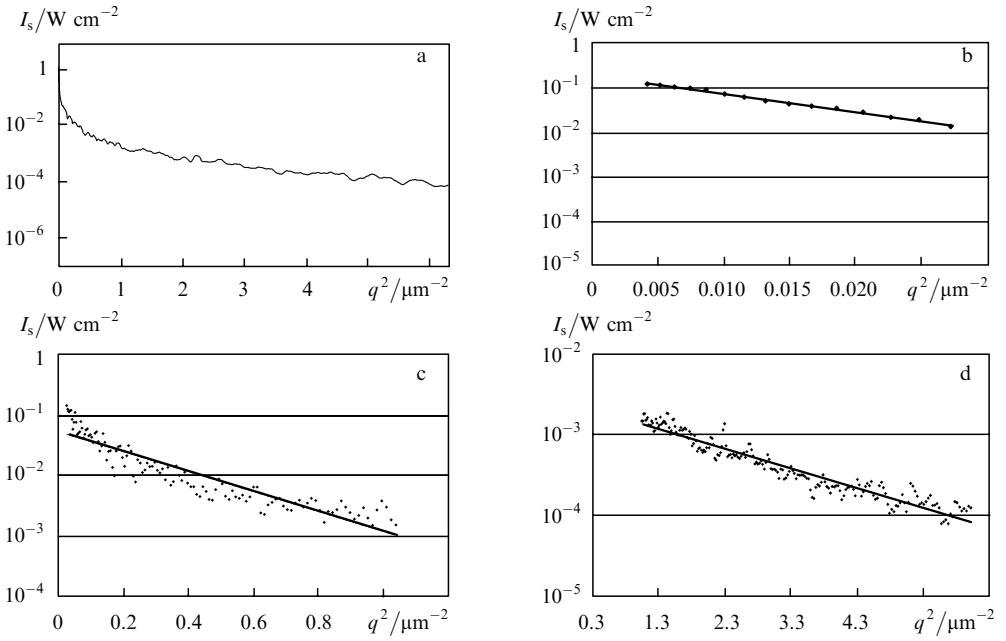

Figure 4. Angular dependences of the scattered radiation intensity in the Guinier coordinates q^2, I_s in the entire angular range (a) and linear approximations of experimental data at separate regions (b–d) for $I = 2 \times 10^5 \exp(-94.1q^2)$, $Q^2 = 0.989$ (b); $I = 522\exp(-3.5q^2)$, $Q^2 = 0.83$ (c); and $I = 24.5\exp(-0.20q^2)$, $Q^2 = 0.83$ (d).

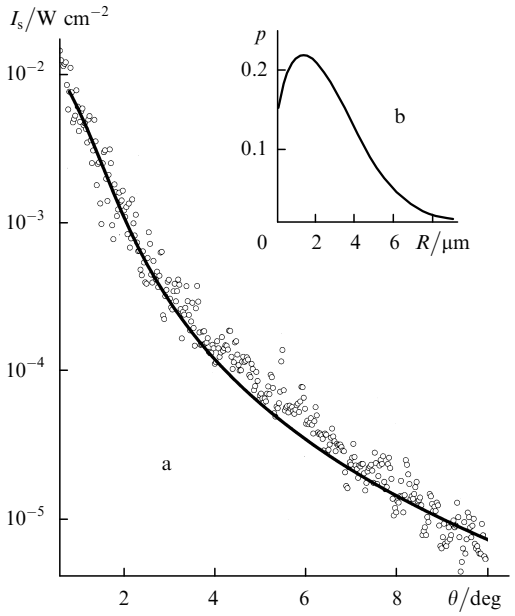

Figure 5. Experimental data and their approximation by (6) with the size distribution of spherical particles (9) for $Q^2 = 0.93$ (a) and distribution (9) for $g = 0.2$ and $d = 4$ μm (b).

function, the additional statistical processing of the results is required, in particular, by using the refined [compared to (6)] mathematical models of the scattering indicatrix for an individual particle, as well as additional experiments, for example, with different probe radiation wavelengths.

4. Conclusions

Our preliminary experiments with laser radiation propagating in twice-distilled water have shown that, despite careful purification, the water contains micron impurities. We have proposed the scheme for studying small-angle scattering of laser radiation in water, which allows the simultaneous investigation of the angular scattering spectrum both at small (less than 0.1°) and large (above 10°) scattering angles. It is shown that the Gaussian profile of a single-mode laser beam propagating through our experimental setup in the absence of the liquid under study is preserved. This allowed us to measure the instrumental function. We have found some parameters of the size distribution function of scatterers from our experimental data. In particular, the maximum of the reconstructed distribution function corresponds to $R = 1.3$ μm. These results confirm indirectly the hypothesis of existence of stable microbubbles of a dissolved gas, bubstons, in pure liquids, which was proposed earlier. In addition, our compact experimental setup can be used for monitoring contamination of reservoirs.

Acknowledgements. This work was supported by the Russian Foundation for Basic Research (Grant Nos 03-02-16589 and 02-02-16184) and the Russian Science Support Foundation.

References

1. Jerlov N.G. *Marine Optics. Elsevier Oceanography Series* (Amsterdam – Oxford – New York: Elsevier Scientific Publ. Comp., 1976) Vol. 14.
2. Carpineti M., Ferri F., Giglio M., Paganini E., Perini U. *Phys. Rev. A*, **42**, 7347 (1990).
3. Giordano R., Mallamace F., Micali M., Wanderlingh F., Baldini G., Doglia S. *Phys. Rev. A*, **28**, 3581 (1983).
4. Bunkin N.F., Bunkin F.V. *Zh. Eksp. Teor. Fiz.*, **101**, 512 (1992).
5. Bunkin N.F., Bunkin F.V. *Zs. Phys. Chem.*, **215**, 111 (2001).
6. Bunkin N.F., Bunkin F.V. *Zh. Eksp. Teor. Fiz.*, **123**, 828 (2003).
7. Bunkin N.F., Bunkin F.V. *Laser Phys.*, **3**, 63 (1993).
8. Bunkin N.F., Lobeev A.V. *Kvantovaya Elektron.*, **21**, 319 (1994) [*Quantum Electron.*, **24**, 297 (1994)].
9. Bunkin N.F., Lobeyev A.V., Mikhalevich V.G. *Phys. Vibrations*, **7**, 205 (1999).
10. Bunkin N.F., Lobeyev A.V., Lyakhov G.A., Ninham B.W. *Phys. Rev. E*, **60**, 1681 (1999).
11. Sankin G.N., Teslenko V.S. *Dokl. Akad. Nauk*, **393**, 762 (2003).
12. Bunkin N.F., Lobeev A.V. *Pis'ma Zh. Eksp. Teor. Fiz.*, **58**, 91 (1993).
13. Bunkin N.F., Lobeyev A.V. *Phys. Lett. A*, **229**, 327 (1997).
14. Svergun D.I., Feigin L.A. *Rentgenovskoe i neitronnoe malouglovoe rasseyanine* (X-ray and Neutron Small-Angle Scattering) (Moscow: Nauka, 1986).
15. Shifrin K.S. *Vvedenie v optiku okeana (Introduction to the Ocean Optics)* (Leningrad: Gidrometeoizdat, 1983).